· Clinical Research ·

Influence of corneal power on circumpapillary retinal nerve fiber layer and optic nerve head measurements by spectral-domain optical coherence tomography

Kazunori Hirasawa[1], Nobuyuki Shoji[2]

[1]Department of Orthoptics and Visual Science, School of Allied Health Sciences, Kitasato University, Sagamihara, Kanagawa 252-0373, Japan
[2]Department of Ophthalmology, School of medicine, Kitasato University, Sagamihara, Kanagawa 252-0373, Japan
Correspondence to: Kazunori Hirasawa. Department of Orthoptics and Visual Science, School of Allied Health Sciences, Kitasato University, 1-15-1 Kitasato, Minami-ku, Sagamihara, Kanagawa 252-0373, Japan. hirasawa@kitasato-u.ac.jp
Received: 2017-02-24 Accepted: 2017-04-24

Abstract
● AIM: To evaluate the influence of corneal power on circumpapillary retinal nerve fiber layer (cpRNFL) and optic nerve head (ONH) measurements by spectral-domain optical coherence tomography (SD-OCT).

● METHODS: Twenty-five eyes of 25 healthy participants (mean age 23.6±3.6y) were imaged by SD-OCT using horizontal raster scans. Disposable soft contact lenses of different powers (from −11 to +5 diopters including 0 diopter) were worn to induce 2-diopter changes in corneal power. Differences in the cpRNFL and ONH measurements per diopter of change in corneal power were analyzed.

● RESULTS: As corneal power increased by 1 diopter, total and quadrant cpRNFL thicknesses, except for the nasal sector, decreased by −0.19 to −0.32 μm (*P*<0.01). Furthermore, the disc, cup, and rim areas decreased by −0.017, −0.007, and −0.015 mm^2, respectively (*P*<0.001); the cup and rim volumes decreased by −0.0013 and −0.006 mm^3, respectively (*P*<0.01); and the vertical and horizontal disc diameters decreased by −0.006 and −0.007 mm, respectively (*P*<0.001).

● CONCLUSION: For more precise OCT imaging, the ocular magnification should be corrected by considering both the axial length and corneal power. However, the effect of corneal power changes on cpRNFL thickness and ONH topography are small when compare with those of the axial length.

● KEYWORDS: optical coherence tomography; ocular magnification; corneal power; circumpapillary retinal nerve fiber layer; optic nerve head

DOI:10.18240/ijo.2017.09.09

Citation: Hirasawa K, Shoji N. Influence of corneal power on circumpapillary retinal nerve fiber layer and optic nerve head measurements by spectral-domain optical coherence tomography. *Int J Ophthalmol* 2017;10(9):1385-1391

INTRODUCTION

Spectral-domain optical coherence tomography (SD-OCT) enables the detection of slight structural changes before visual field deterioration in early glaucoma[1-14]. Such changes are difficult to detect by traditional ophthalmoscopy or fundus photography. However, measurements of structures such as the circumpapillary retinal nerve fiber layer (cpRNFL) and optic nerve head (ONH) are influenced by factors including axial length and high myopia independently of the degree of glaucomatous change[13,15-27]. Therefore, these measurements should be corrected according to the individual's ocular magnification for accuracy.

Traditionally, Littmann's[28] formula and Bennett *et al*'s[29] modification are used to correct for ocular magnification, as follows: $t=p\times q\times s$, where t is the actual fundus dimension, p is the magnification factor of the camera of the imaging system, q is the magnification factor of the individual eye, and s is the value obtained from the imaging device. Factor p is a constant in a telecentric system. Factor q can be determined by the following formula[29]: q=0.01306×(axial length −1.82). Nevertheless, these formulas do not consider the optical properties of the anterior segment, particularly the corneal power, because the position of the second principal point is assumed constant. Researchers have investigated the influence of corneal power on cpRNFL measurements by SD-OCT[30-32], but their findings are not consistent. In addition, previous studies did not analyze the effect on ONH measurements. In this study, we evaluated the influence of corneal power on cpRNFL and ONH measurements by SD-OCT.

SUBJECTS AND METHODS

This cross sectional study followed the tenets of the Declaration of Helsinki. Written informed consent was obtained from each participant after approval was received from the Ethics Committee of Kitasato University School of Allied Health

Science (No.2015-07). UMIN clinical trials registry (http://www.umin.ac.jp/) under unique trial number UMIN000016698 (date of registration: 03/03/2015).

Twenty-five healthy participants (mean age 23.6±3.6y, 3 males) underwent comprehensive ophthalmic examinations, including noncycloplegic refraction testing, visual acuity testing at 5 m using a Landolt ring chart, intraocular pressure and axial length measurements, and slit-lamp and fundus examinations, by a glaucoma specialist (Shoji N). For each participant, the eye with a corrected visual acuity of 20/20 or better, intraocular pressure of 21 mm Hg or lower, and more normal optic disc appearance was included in the study. If both eyes met these inclusion criteria, the eye with lower astigmatism was included.

The cpRNFL thickness and ONH topography were measured by an SD-OCT system (3D OCT-2000, version 8.1.1; Topcon, Tokyo, Japan) using the 3D optic disc horizontal raster scan mode with a 512×128 scan resolution and 6 mm^2 scan area. This device operates at a speed of 50 000 A-scans per second and has a depth and lateral resolution of 6 μm and 20 μm or less, respectively. It requires a pupil size of 2.5 mm or larger for imaging. Although the device can correct for ocular magnification on the basis of Littmann's[28] formula ocular magnification was not corrected in this study.

A single expert examiner (Hirasawa K) performed all of the measurements in the selected eyes without cycloplegia. The participants wore 10 differently powered (from -11 to +5 diopters including plano) disposable soft contact lenses (1-day Acuvue, Johnson & Johnson Vision Care, Inc., New Brunswick, NJ, USA) in random order to change the corneal power, which was measured with an auto kerato-refractometer (KR-8100PA, Topcon) before SD-OCT. When the signal strength was unacceptable by over 40 at each contact lens power or when B-scan line images were absent or deviated because of movement, the imaging was repeated up to twice for each imaging. The following parameters were evaluated: total and quadrant cpRNFL thicknesses, centered on the optic disc; disc, cup, and rim areas; cup and rim volumes; vertical and horizontal disc diameters; and image quality.

Statistical Analysis All data were analyzed using *R* software (http://www.R-project.org) and G*Power3 version 3.1.7[33-34]. The effect size, α error, power (1-β error), and nonsphericity correction were 0.25 (middle), 0.05, 0.95, and 0.12, respectively, and the required sample size was 11 participants for 10 repeated measurements[35]. Using three sets of measurements obtained with plano contact lenses, the repeatability was calculated by the Bland and Altman method[36-37] as 2.77×Sw. Sw is the within-subject standard deviation and formula is as follows:

Within subject standard deviation (Sw)= $\sqrt{\frac{\sum SD_i^2}{n}}$

where SD_i^2 is the standard deviation of measurements on each subject, where n is the number of participants. Intraclass correlation coefficients were also calculated. When the confidence limit on either side of the estimate of Sw was set to 0.20, the required sample size was 24 eyes.

The first set of measurements were obtained with plano contact lenses, and data collected without a contact lens were compared by the paired *t*-test to analyze the effect of contact lens wearing on cpRNFL and ONH measurements. Differences of cpRNFL thickness and ONH parameter with different powers of contact lenses were analyzed by repeated-measures analysis of variance.

RESULTS

In this study, 15 right and 10 left eyes were imaged. Table 1 shows their initial optical characteristics.

Contact lens wearing did not significantly affect the cpRNFL and ONH measurements (Table 2) or their repeatability (Table 3).

As shown in Table 4, the measured cpRNFL thickness in every region except for the nasal sector, ONH parameters, and image quality significantly differed with varying contact lens powers

Table 1 Ocular characteristics of the participants

Parameters	Mean±SD	Range
Spherical power (diopter)	−3.59±3.08	−7.87 to 4.50
Astigmatic power (diopter)	−0.49±0.27	−1.00 to 0.00
Spherical equivalent (diopter)	−3.84±3.10	−8.12 to 4.25
Corneal curvature (mm)	7.84±0.26	7.38 to 8.32
Corneal power (diopter)	43.15±1.45	40.62 to 45.87
Visual acuity (logMAR)	−0.14±0.08	−0.28 to 0.04
Intraocular pressure (mm Hg)	14.5±2.2	9.1 to 19.7
Axial length (mm)	24.82±1.42	21.96 to 28.29

Table 2 Measurements of cpRNFL thickness and ONH topography with plano soft contact lens

Parameters	Without lens	With lens	*P*
cpRNFL thickness (μm)			
Total	103.7±7.6	104.0±8.1	0.367
Temporal	90.6±15.1	91.0±15.9	0.525
Superior	124.1±13.5	123.5±14.3	0.420
Nasal	71.0±13.4	71.8±14.2	0.292
Inferior	129.2±15.0	129.8±15.8	0.393
ONH topography			
Disc area (mm^2)	2.39±0.47	2.41±0.46	0.139
Cup area (mm^2)	0.68±0.45	0.75±0.49	0.098
Rim area (mm^2)	1.71±0.43	1.66±0.46	0.252
Cup volume (mm^3)	0.12±0.14	0.13±0.14	0.574
Rim volume (mm^3)	0.62±0.32	0.59±0.31	0.153
Vertical disc diameter (mm)	1.83±0.17	1.82±0.17	0.822
Horizontal disc diameter (mm)	1.67±0.20	1.69±0.20	0.107
Image quality	55.4±3.5	55.8±3.7	0.227

cpRNFL: Circumpapillary retinal nerve fiber layer; ONH: optic nerve head. Data represent mean±SD, Sw, and 2.77×Sw.

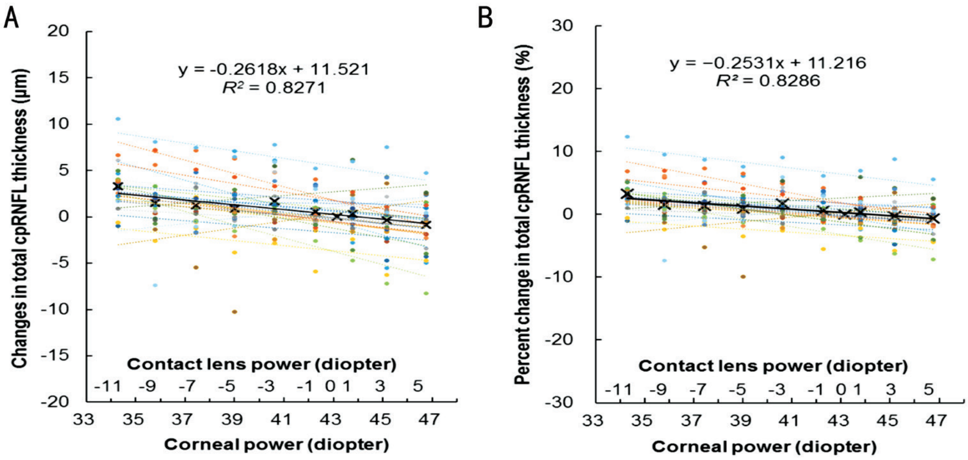

Figure 1 Actual (A) and percent (B) changes in total cpRNFL thickness induced by increasing corneal power using soft contact lenses.

Table 3 Repeatability of the measurements with plano soft contact lenses

Parameters	Repeatability		
	Sw (2.77×Sw)	ICC (95% CI)	*P*
cpRNFL thickness (μm)			
Total	1.9 (5.3)	0.979 (0.959, 0.990)	<0.0001
Temporal	3.1 (8.6)	0.993 (0.985, 0.996)	<0.0001
Superior	4.1 (11.3)	0.969 (0.940, 0.985)	<0.0001
Nasal	5.0 (13.9)	0.963 (0.928, 0.982)	<0.0001
Inferior	4.0 (11.1)	0.976 (0.953, 0.989)	<0.0001
ONH topography			
Disc area (mm^2)	0.09 (0.25)	0.992 (0.985, 0.996)	<0.0001
Cup area (mm^2)	0.20 (0.56)	0.939 (0.881, 0.971)	<0.0001
Rim area (mm^2)	0.19 (0.53)	0.932 (0.868, 0.968)	<0.0001
Cup volume (mm^3)	0.02 (0.06)	0.999 (0.998, 1.000)	<0.0001
Rim volume (mm^3)	0.09 (0.24)	0.978 (0.957, 0.989)	<0.0001
Vertical disc diameter (mm)	0.05 (0.13)	0.977 (0.955, 0.989)	<0.0001
Horizontal disc diameter (mm)	0.07 (0.18)	0.978 (0.958, 0.990)	<0.0001
Image quality	2.1 (5.7)	0.896 (0.797, 0.951)	<0.0001

cpRNFL: Circumpapillary retinal nerve fiber layer; ONH: Optic nerve head; Sw: Within-subject standard deviation; ICC: Intraclass correlation; CI: Confidence interval.

(repeated-measures analysis of variance, P<0.05). The changes in total cpRNFL thickness with 2-diopter induced increases in corneal power are depicted in Figure 1.

The different colored dots and their approximating lines indicate data from individual participants. The crosses and solid line indicate the mean data of all the participants.

Table 5 shows that the total cpRNFL thickness significantly decreased by −0.26 μm (−0.25%, P<0.001) and the quadrant cpRNFL thickness, with the exception of the nasal sector, significantly decreased by −0.19 to −0.32 μm (−0.17% to −0.25%, all P<0.007) as the corneal power increased by 1 diopter. All ONH measurements also significantly decreased with the 1-diopter-induced increases in corneal power (P<0.001). Only the image quality increased (0.2 or 0.36% per diopter) with increasing corneal power (P=0.007).

DISCUSSION

This study demonstrated good repeatability of the measurements with and without a contact lens. Therefore, contact lens wearing does not introduce bias in SD-OCT imaging. However, image quality reduces with induced decreases in corneal power, in turn affecting assessment of cpRNFL thickness[38-39]. The current data might include bias where image quality is concerned.

The total and quadrant cpRNFL thicknesses, except for nasal region, showed up to 0.3 μm decreases (−0.4%), and ONH area measurements were reduced up to 1.1% per diopter induced increase in corneal power. One study showed that the total cpRNFL thickness measured by time-domain OCT does not significantly differ with varying corneal power[32], whereas another study demonstrated that cpRNFL thickness measured

Table 4 Changes in the measurements with increasing soft contact lens power mean±SD

Parameters	Contact lens power (diopter)										^aP
	−11	−9	−7	−5	−3	−1	0	+1	+3	+5	
Corneal power (diopter)	34.29±1.54	35.79±1.47	37.43±1.59	39.01±1.67	40.62±1.55	42.27±1.69	43.15±1.45	43.79±1.37	45.17±1.63	46.76±1.43	<0.0001
cpRNFL thickness (μm)											
Total	106.4±8.0	104.6±8.3	104.4±4.4	104.0±4.0	104.8±4.8	103.7±3.7	103.1±8.2	103.4±3.4	102.8±7.5	102.3±7.1	<0.0001
Temporal	92.4±15.1	91.5±14.9	90.8±14.5	91.8±15.2	90.8±13.9	89.3±14.4	89.4±14.6	89.2±15.5	89.2±14.3	88.6±13.9	0.003
Superior	124.6±12.9	124.7±12.6	123.8±23.8	122.9±22.9	124.5±24.5	124.2±24.2	123.2±23.2	122.8±22.8	122.8±22.8	121.6±21.6	0.021
Nasal	74.0±16.4	70.5±0.5	70.1±15.4	71.3±1.3	72.4±2.4	71.2±1.2	70.2±0.2	72.1±2.1	71.3 ± 1.3	70.9±0.9	0.236
Inferior	134.1±34.1	131.8±31.8	132.5±32.5	130.1±30.1	131.5±31.5	130.1±30.1	129.6±29.6	129.6±29.6	129.4±29.4	130.1±30.1	<0.0001
ONH topography											
Disc area (mm^2)	2.56±0.53	2.50±0.50	2.46±0.46	2.48±0.48	2.43±0.43	2.35±0.35	2.37±.0.45	2.37±0.37	2.36±0.36	2.34±0.34	<0.0001
Cup area (mm^2)	0.75±0.50	0.71±0.71	0.71±0.71	0.70±0.70	0.69±0.69	0.66±0.66	0.67±0.67	0.66±0.66	0.66±0.66	0.65±0.65	<0.0001
Rim area (mm^2)	1.83±0.83	1.79±0.79	1.75±0.75	1.79±0.79	1.74±0.74	1.69±0.69	1.71±0.71	1.71±0.61	1.66±0.66	1.68±0.68	<0.0001
Cup volume (mm^3)	0.15±0.15	0.14±0.14	0.14±0.14	0.14±0.14	0.13±0.13	0.13±0.13	0.13±0.13	0.13±0.13	0.13±0.13	0.13±0.13	<0.0001
Rim volume (mm^3)	0.66±0.37	0.65±0.65	0.64±0.64	0.63±0.63	0.63±0.63	0.61±0.61	0.62±0.62	0.56±0.56	0.57±0.57	0.61±0.61	0.101
Vertical disc diameter (mm)	1.88±0.88	1.87±0.87	1.84±0.84	1.86±0.86	1.84±0.84	1.81±0.81	1.83±0.83	1.82±0.82	1.81±0.81	1.82±0.82	<0.0001
Horizontal disc diameter (mm)	1.73±0.73	1.70±0.70	1.69±0.69	1.70±0.70	1.68±0.68	1.66±0.66	1.66±0.66	1.66±0.66	1.65±0.65	1.64±0.64	<0.0001
Image quality	53.3±4.3	52.4±2.4	53.1±3.1	54.7±4.7	55.4±5.4	54.9±4.9	54.5±4.5	55.3±5.3	55.1±5.1	54.7±4.7	<0.0001

cpRNFL: Circumpapillary retinal nerve fiber layer; ONH: Optic nerve head. ^aP<0.05 is statistically significant by repeated-measure analysis of variance.

Table 5 Slope values of actual and percent changes in the measurements per diopter increase in corneal power

Parameters	Actual change (diopter)				Percent change (diopter)			
	Slope	95% CI	R^2	P	Slope	95% CI	R^2	^aP
cpRNFL thickness (μm)								
Total	−0.26	−0.36, −0.16	0.827	<0.0001	−0.25	−0.35, −0.16	0.829	<0.0001
Temporal	−0.30	−0.39, −0.21	0.882	<0.0001	−0.35	−0.45, −0.24	0.877	<0.0001
Superior	−0.19	−0.32, −0.07	0.615	0.007	−0.17	−0.26, −0.07	0.682	0.003
Nasal	−0.08	−0.31, 0.14	0.086	0.412	−0.06	−0.41, 0.30	0.018	0.711
Inferior	−0.32	−0.48, −0.16	0.726	0.001	−0.25	−0.38, −0.12	0.716	0.002
ONH topography								
Disc area (mm^2)	−0.017	−0.022, −0.013	0.904	<0.0001	−0.71	−0.22, −0.01	0.893	<0.0001
Cup area (mm^2)	−0.007	−0.009, −0.005	0.914	<0.0001	−1.13	−1.42, −0.84	0.914	<0.0001
Rim area (mm^2)	−0.015	−0.021, 0.0008	0.765	<0.0001	−0.78	−1.09, −0.48	0.818	<0.0001
Cup volume (mm^3)	−0.0013	−0.0018, −0.0008	0.844	<0.0001	−1.08	−1.65, −0.50	0.699	0.002
Rim volume (mm^3)	−0.006	−0.010, 0.003	0.645	0.005	−0.80	−1.18, −0.42	0.749	0.001
Vertical disc diameter (mm)	−0.006	−0.008, −0.003	0.783	<0.0001	−0.31	−0.44, −0.17	0.778	<0.0001
Horizontal disc diameter (mm)	−0.007	−0.008, −0.005	0.940	<0.0001	−0.40	−0.49, −0.32	0.937	<0.0001
Image quality	0.20	0.07, 0.34	0.615	0.007	0.36	0.12, 0.60	0.608	0.007

cpRNFL: Circumpapillary retinal nerve fiber layer; ONH: Optic nerve head; CI: Confidence interval. ^aP<0.05 is statistically significant by simple linear regression analysis.

by SD-OCT decreases by approximately 0.5 μm (−0.5%) per diopter induced increase in corneal power[30-31]. Positional variation of the second principal point due to changes in corneal power would affect cpRNFL and ONH measurements. In Littmann's formula modified by Bennett *et al*[29], the second principal point is assumed to be located at 1.82 mm from the corneal surface based on Bennett and Rabbetts' schematic eye[40]. However, its position moves backward and forward when the corneal power becomes steeper and flatter, respectively, because the calculation is based on the principal point of the crystalline lens, corneal power, and total ocular power, as follows[40]:

$$\overline{P_{lens}'P_{eye}'} = \frac{(n_{vitreous})\ (P_{cornea}'P_{lens}')\ (F_{ec})}{(n_{aqueous})\ (F_{eeye})}$$

$$\overline{A_{cornea}\ P_{eye}'} = \overline{A_{cornea}\ P_{lens}'} + \overline{P_{lens}'\ P_{eye}'}$$

Where P_{lens}' is the second principal plane of the crystalline lens, P_{eye}' is the second principal plane of the eye, $\overline{P_{lens}'\ P_{eye}'}$ is the distance from the second principal plane of the crystalline lens to the second principal plane of the eye, $n_{vitreous}$ is the refractive index of the vitreous body, $P_{cornea}'P_{lens}'$ is the distance from the second principal plane of the cornea to the second principal plane of the crystalline lens, F_{ec} is the equivalent power of the cornea, $n_{aqueous}$ is the refractive index of the aqueous humor, F_{eye} is the equivalent power of the eye, A_{cornea} is the anterior surface of the cornea, and $\overline{A_{cornea}P_{eye}'}$ is the distance from the anterior surface of the cornea to the second principal plane of the eye (second principal point). By substituting the variation value of corneal power in the current study and other parameters based on Bennett and Rabbetts' schematic eye[40] into these formulas, the second principal point position ranges from 2.67 to 1.46. As a result, the *q* value in Littmann's formula modified by Bennett *et al*[29], which expresses the magnification factor of the individual eye, varies by -0.0048 (-1.6%) to 0.0111 (+3.8%) compared to average axial length of 24.39 mm and the second principal point of 1.82 mm. Therefore, the apparent ONH size on a fundus photograph might be slightly decreased with induced increases in corneal power, decreasing cpRNFL and ONH measurements. However, the second principal point position was calculated with approximate value based on the schematic eyes, not actually measured in each participant. Further study is needed using the actual value in each participant.

A slight difference in cpRNFL thickness was noted between the previous (−0.4 to −0.5 μm/diopter)[30-31] and the current (−0.2 to −0.3 μm/diopter) studies. This difference can be attributed to the control of accommodative effects by cycloplegic eye drops. Although cycloplegic eye drops were used to control pupil size and accommodation in previous studies[30-31], the cpRNFL and ONH were imaged without cycloplegia in the current study. The anterior pole of the lens moves anteriorly by 0.05 mm/diopter of accommodation, while the posterior pole moves slightly back by 0.01 mm/diopter; thus, the center of the lens moves forward by 0.02 mm/diopter. This means that 0.24 mm of the 1.2 mm range of the second principal point change may be a direct result of the lens anterior shift as a consequence of the accommodation in this study. Further, the position of the second principal point would have varied slightly due to accommodation that occurred when the corneal power was decreased by using the contact lenses with a high negative power.

Previous studies showed that measured cpRNFL thickness without correction for ocular magnification decreases in the range of −1.8 to −4.8 μm as the 1-mm axial length increases[13,15-17,19,21-22,25,27]. These slope values can be converted to −0.6 to −1.6 per diopter using a ratio of 1 mm axial length to 3-diopter refractive error based on a three-surface schematic eye[40]. In addition, the measured disc area without correction for ocular magnification becomes smaller by −0.72 mm^2 as myopia increases by 1 diopter[26]. Although the results cannot be directly compared because the previous data are based on interindividual comparisons[13,15-17,19,21-22,25-27], they suggest that the influence of corneal power on cpRNFL and ONH measurements is less than that of axial length.

There was no difference in cpRNFL thickness in the nasal region induced by an increase in corneal power. The magnitude of curvature in this region is generally larger than that of the temporal, superior, or inferior region, especially considering the longer axial length of a myopic eye. The cpRNFL thickness was measured by the same scan circle size. When the fundus image is magnified by the induced increase in corneal power, the scan area at the nasal region is smaller than that of the temporal, superior, or inferior region. No difference in cpRNFL thickness at the nasal region could be attributed to the magnitude of curvature of the fundus since the scan circle is centered on the optic disc.

Research on refractive surgeries for myopia such as laser-assisted *in situ* keratomileusis[41-45], small incision lenticule extraction[46-51], and phakic intraocular lens implantation[52-54] has been performed worldwide. Although these procedures could change the position of the second principal point, a previous report indicated that refractive surgery does not affect the measured cpRNFL thickness[55-57]. A reason for this finding is that ocular magnification does not change considerably because the cornea is minimally resected. However, careful attention is required for ocular magnification when the corneal resection volume is large.

In summary, induced changes in corneal power lead to decreased cpRNFL and ONH measurements in SD-OCT. For more precise OCT imaging, the ocular magnification should be corrected by considering the individual axial length and second principal point position. However, the conventional magnification correction based on Littmann's formula modified by Bennett *et al*[29] is adequate for daily clinical imaging because the apparent changes in cpRNFL thickness and ONH topography due to corneal power changes are small when compared with those due to axial length.

ACKNOWLEDGEMENTS

Foundation: Supported by a Research Fund at Kitasato University.

Conflicts of Interest: Hirasawa K, None; **Shoji N,** None.

REFERENCES

1 Leung CK, Cheung CY, Weinreb RN, Qiu Q, Liu S, Li H, Xu G, Fan N, Huang L, Pang CP, Lam DS. Retinal nerve fiber layer imaging with spectral-domain optical coherence tomography: a variability and diagnostic performance study. *Ophthalmology* 2009;116(7):1257-1263, 1263.e1-e2.

2 Mwanza JC, Chang RT, Budenz DL, Durbin MK, Gendy MG, Shi W, Feuer WJ. Reproducibility of peripapillary retinal nerve fiber layer thickness and optic nerve head parameters measured with cirrus HD-OCT in glaucomatous eyes. *Invest Ophthalmol Vis Sci* 2010;51(11):5724-5730.

3 Garcia-Martin E, Pinilla I, Idoipe M, Fuertes I, Pueyo V. Intra and interoperator reproducibility of retinal nerve fibre and macular thickness measurements using Cirrus Fourier-domain OCT. *Acta Ophthalmol* 2011; 89(1):e23-e29.

4 Kim JS, Ishikawa H, Sung KR, Xu J, Wollstein G, Bilonick RA, Gabriele ML, Kagemann L, Duker JS, Fujimoto JG, Schuman JS. Retinal nerve fibre layer thickness measurement reproducibility improved with spectral domain optical coherence tomography. *Br J Ophthalmol* 2009;93(8):1057-1063.

5 Carpineto P, Nubile M, Agnifili L, Toto L, Aharrh-Gnama A, Mastropasqua R, Di Antonio L, Fasanella V, Mastropasqua A. Reproducibility and repeatability of Cirrus^{TM} HD-OCT peripapillary retinal nerve fibre layer thickness measurements in young normal subjects. *Ophthalmologica* 2012;227(3):139-145.

6 Tan BB, Natividad M, Chua KC, Yip LW. Comparison of retinal nerve fiber layer measurement between 2 spectral domain OCT instruments. *J Glaucoma* 2012;21(4):266-273.

7 Wu H, de Boer JF, Chen TC. Reproducibility of retinal nerve fiber layer thickness measurements using spectral domain optical coherence tomography. *J Glaucoma* 2011;20(8):470-476.

8 Gonzalez-Garcia AO, Vizzeri G, Bowd C, Medeiros FA, Zangwill LM, Weinreb RN. Reproducibility of RTVue retinal nerve fiber layer thickness and optic disc measurements and agreement with Stratus optical coherence tomography measurements. *Am J Ophthalmol* 2009;147(6):1067-1074, 1074.e1061.

9 Garas A, Vargha P, Hollo G. Reproducibility of retinal nerve fiber layer and macular thickness measurement with the RTVue-100 optical coherence tomograph. *Ophthalmology* 2010;117(4):738-746.

10 Nakatani Y, Higashide T, Ohkubo S, Takeda H, Sugiyama K. Evaluation of macular thickness and peripapillary retinal nerve fiber layer thickness for detection of early glaucoma using spectral domain optical coherence tomography. *J Glaucoma* 2011;20(4):252-259.

11 Lee SH, Kim SH, Kim TW, Park KH, Kim DM. Reproducibility of retinal nerve fiber thickness measurements using the test-retest function of spectral OCT/SLO in normal and glaucomatous eyes. *J Glaucoma* 2010; 19(9):637-642.

12 Mansoori T, Viswanath K, Balakrishna N. Reproducibility of peripapillary retinal nerve fibre layer thickness measurements with spectral domain optical coherence tomography in normal and glaucomatous eyes. *Br J Ophthalmol* 2011;95(5):685-688.

13 Hirasawa K, Shoji N, Yoshii Y, Haraguchi S. Determination of axial length requiring adjustment of measured circumpapillary retinal nerve fiber layer thickness for ocular magnification. *PLoS One* 2014;9(9):e107553.

14 Miki A, Medeiros FA, Weinreb RN, Jain S, He F, Sharpsten L, Khachatryan N, Hammel N, Liebman JM, Girkin CA, Sample PA, Zengwill LM. Rates of retinal nerve fiber layer thinning in glaucoma suspect eyes. *Ophthalmology* 2014;121(7):1350-1358.

15 Leung CK, Mohamed S, Leung KS, Cheung CY, Chan SL, Cheng DK, Lee AK, Leung GY, Rao SK, Lam DS. Retinal nerve fiber layer measurements in myopia: an optical coherence tomography study. *Invest Ophthalmol Vis Sci* 2006;47(12):5171-5176.

16 Budenz DL, Anderson DR, Varma R, Schuman J, Cantor L, Savell J, Greenfield DS, Patella VM, Quigley HA, Tielsch J. Determinants of normal retinal nerve fiber layer thickness measured by Stratus OCT. *Ophthalmology* 2007;114(6):1046-1052.

17 Hougaard JL, Ostenfeld C, Heijl A, Bengtsson B. Modelling the normal retinal nerve fibre layer thickness as measured by Stratus optical coherence tomography. *Graefes Arch Clin Exp Ophthalmol* 2006; 244(12):1607-1614.

18 Kim MJ, Lee EJ, Kim TW. Peripapillary retinal nerve fibre layer thickness profile in subjects with myopia measured using the Stratus optical coherence tomography. *Br J Ophthalmol* 2010;94(1):115-120.

19 Bendschneider D, Tornow RP, Horn FK, Laemmer R, Roessler CW, Juenemann AG, Kruse FE, Mardin CY. Retinal nerve fiber layer thickness in normals measured by spectral domain OCT. *J Glaucoma* 2010;19(7):475-482.

20 Cheung CY, Chen D, Wong TY, Tham YC, Wu R, Zheng Y, Cheng CY, Saw SM, Baskaran M, Leung CK, Aung T. Determinants of quantitative optic nerve measurements using spectral domain optical coherence tomography in a population-based sample of non-glaucomatous subjects. *Invest Ophthalmol Vis Sci* 2011;52(13):9629-9635.

21 Yoo YC, Lee CM, Park JH. Changes in peripapillary retinal nerve fiber layer distribution by axial length. *Optom Vis Sci* 2012;89(1):4-11.

22 Huang D, Chopra V, Lu AT, Tan O, Francis B, Varma R. Advanced Imaging for Glaucoma Study-AIGS Group. Does optic nerve head size variation affect circumpapillary retinal nerve fiber layer thickness measurement by optical coherence tomography? *Invest Ophthalmol Vis Sci* 2012;53(8):4990-4997.

23 Aykut V, Oner V, Tas M, Iscan Y, Agachan A. Influence of axial length on peripapillary retinal nerve fiber layer thickness in children: a study by RTVue spectral-domain optical coherence tomography. *Curr Eye Res* 2013;38(12):1241-1247.

24 Oner V, Aykut V, Tas M, Alakus MF, Iscan Y. Effect of refractive status on peripapillary retinal nerve fibre layer thickness: a study by RTVue spectral domain optical coherence tomography. *Br J Ophthalmol* 2013;97(1):75-79.

25 Kang SH, Hong SW, Im SK, Lee SH, Ahn MD. Effect of myopia on the thickness of the retinal nerve fiber layer measured by Cirrus HD optical coherence tomography. *Invest Ophthalmol Vis Sci* 2010;51(8): 4075-4083.

26 Savini G, Barboni P, Parisi V, Carbonelli M. The influence of axial length on retinal nerve fibre layer thickness and optic-disc size measurements by spectral-domain OCT. *Br J Ophthalmol* 2012;96(1):57-61.

27 Hirasawa K, Shoji N, Yoshii Y, Haraguchi S. Comparison of Kang's and Littmann's methods of correction for ocular magnification in circumpapillary retinal nerve fiber layer measurement. *Invest Ophthalmol Vis Sci* 2014;55(12):8353-8358.

28 Littmann H. Determination of the real size of an object on the fundus of the living eye. *Klin Monbl Augenheilkd* 1982;180(4):286-289.

29 Bennett AG, Rudnicka AR, Edgar DF. Improvements on Littmann's method of determining the size of retinal features by fundus photography. *Graefes Arch Clin Exp Ophthalmol* 1994;232(6):361-367.

30 Lee J, Kim NR, Kim H, Han J, Lee ES, Seong GJ, Kim CY. Negative refraction power causes underestimation of peripapillary retinal nerve fibre layer thickness in spectral-domain optical coherence tomography. *Br J Ophthalmol* 2011;95(9):1284-1289.

31 Patel NB, Garcia B, Harwerth RS. Influence of anterior segment power on the scan path and RNFL thickness using SD-OCT. *Invest Ophthalmol Vis Sci* 2012;53(9):5788-5798.

32 Salchow DJ, Hwang AM, Li FY, Dziura J. Effect of contact lens power on optical coherence tomography of the retinal nerve fiber layer. *Invest Ophthalmol Vis Sci* 2011;52(3):1650-1654.

33 Faul F, Erdfelder E, Buchner A, Lang AG. Statistical power analyses using G*Power 3.1: tests for correlation and regression analyses. *Behav Res Methods* 2009;41(4):1149-1160.

34 Faul F, Erdfelder E, Lang AG, Buchner A. G*Power 3: a flexible statistical power analysis program for the social, behavioral, and biomedical sciences. *Behav Res Methods* 2007;39(2):175-191.

35 Cohen J. Statistical power analysis for the behavioral sciences. Second Edition. Hillsdale, New Jersey: Lawrence Erlbaum Associates, 1988.

36 Bland JM, Altman DG. Measurement error proportional to the mean. *BMJ* 1996;313(7049):106.

37 Bland JM, Altman DG. Measurement error. *BMJ* 1996;313(7059):744.

38 Cheung CY, Leung CK, Lin D, Pang CP, Lam DS. Relationship between retinal nerve fiber layer measurement and signal strength in optical coherence tomography. *Ophthalmology* 2008;115(8):1347-1351, 1351.e1-e2.

39 Ha MM, Kim JM, Kim HJ, Park KH, Kim M, Choi CY. Low limit for effective signal strength in the Stratus OCT in imperative low signal strength cases. *Korean J Ophthalmol* 2012;26(3):182-188.

40 Rabbett RB. Bennett and Rabbetts' Clinical Visual Optics. 4th Edition. Oxford: Butterworth-Heinemann, 2007.

41 Aizawa D, Shimizu K, Komatsu M, Ito M, Suzuki M, Ohno K, Uozato H. Clinical outcomes of wavefront-guided laser in situ keratomileusis: 6-month follow-up. *J Cataract Refract Surg* 2003;29(8):1507-1513.

42 Igarashi A, Kamiya K, Shimizu K, Komatsu M. Visual performance after implantable collamer lens implantation and wavefront-guided laser in situ keratomileusis for high myopia. *Am J Ophthalmol* 2009;148(1):164-170.e1.

43 Igarashi A, Kamiya K, Shimizu K, Komatsu M. Time course of refractive and corneal astigmatism after laser in situ keratomileusis for moderate to high astigmatism. *J Cataract Refract Surg* 2012;38(8):1408-1413.

44 Kamiya K, Shimizu K, Igarashi A, Komatsu M. Comparison of Collamer toric implantable [corrected] contact lens implantation and wavefront-guided laser in situ keratomileusis for high myopic astigmatism. *J Cataract Refract Surg* 2008;34(10):1687-1693.

45 Kobashi H, Kamiya K, Igarashi A, Matsumura K, Komatsu M, Shimizu K. Long-term quality of life after posterior chamber phakic intraocular lens implantation and after wavefront-guided laser in situ keratomileusis for myopia. *J Cataract Refract Surg* 2014;40(12):2019-2024.

46 Ishii R, Shimizu K, Igarashi A, Kobashi H, Kamiya K. Influence of femtosecond lenticule extraction and small incision lenticule extraction on corneal nerve density and ocular surface: a 1-year prospective, confocal, microscopic study. *J Refract Surg* 2015;31(1):10-15.

47 Kamiya K, Shimizu K, Igarashi A, Kobashi H. Visual and refractive outcomes of femtosecond lenticule extraction and small-incision lenticule extraction for myopia. *Am J Ophthalmol* 2014;157(1):128-134.e2.

48 Kamiya K, Shimizu K, Igarashi A, Kobashi H. Effect of femtosecond laser setting on visual performance after small-incision lenticule extraction for myopia. *Br J Ophthalmol* 2015;99(10):1381-1387.

49 Kamiya K, Shimizu K, Igarashi A, Kobashi H, Sato N, Ishii R. Intraindividual comparison of changes in corneal biomechanical parameters after femtosecond lenticule extraction and small-incision lenticule extraction. *J Cataract Refract Surg* 2014;40(6):963-970.

50 Kobashi H, Kamiya K, Ali MA, Igarashi A, Elewa ME, Shimizu K. Comparison of astigmatic correction after femtosecond lenticule extraction and small-incision lenticule extraction for myopic astigmatism. *PLoS One* 2015;10(4):e0123408.

51 Sekundo W, Kunert KS, Blum M. Small incision corneal refractive surgery using the small incision lenticule extraction (SMILE) procedure for the correction of myopia and myopic astigmatism: results of a 6 month prospective study. *Br J Ophthalmol* 2011;95(3):335-339.

52 Igarashi A, Shimizu K, Kamiya K. Eight-year follow-up of posterior chamber phakic intraocular lens implantation for moderate to high myopia. *Am J Ophthalmol* 2014;157(3):532-539.e1.

53 Kamiya K, Shimizu K, Igarashi A, Kobashi H. Factors influencing long-term regression after posterior chamber phakic intraocular lens implantation for moderate to high myopia. *Am J Ophthalmol* 2014;158(1):179-184.e1.

54 Kamiya K, Shimizu K, Kobashi H, Igarashi A, Komatsu M, Nakamura A, Kojima T, Nakamura T. Three-year follow-up of posterior chamber toric phakic intraocular lens implantation for the correction of high myopic astigmatism in eyes with keratoconus. *Br J Ophthalmol* 2015;99(2):177-183.

55 Gurses-Ozden R, Liebmann JM, Schuffner D, Buxton DF, Soloway BD, Ritch R. Retinal nerve fiber layer thickness remains unchanged following laser-assisted in situ keratomileusis. *Am J Ophthalmol* 2001;132(4):512-516.

56 Sharma N, Sony P, Gupta A, Vajpayee RB. Effect of laser in situ keratomileusis and laser-assisted subepithelial keratectomy on retinal nerve fiber layer thickness. *J Cataract Refract Surg* 2006;32(3):446-450.

57 Zangwill LM, Abunto T, Bowd C, Angeles R, Schanzlin DJ, Weinreb RN. Scanning laser polarimetry retinal nerve fiber layer thickness measurements after LASIK. *Ophthalmology* 2005;112(2):200-207.